



Published in final edited form as:

*Int J Radiat Oncol Biol Phys.* 2022 February 01; 112(2): 542–553. doi:10.1016/j.ijrobp.2021.09.025.

## A novel role for RNF126 in the promotion of G2 arrest via interaction with 14–3–3 $\sigma$

Pengyan Fa, M.S.<sup>1</sup>, Zhaojun Qiu, Ph.D.<sup>1</sup>, Qi-En Wang, Ph.D.<sup>1</sup>, Chunhong Yan, Ph.D.<sup>2</sup>, Junran Zhang, M.D., Ph.D.<sup>1,\*</sup>

<sup>1</sup>Department of Radiation Oncology, The Ohio State University James Comprehensive Cancer Center and College of Medicine, OH, USA

<sup>2</sup>Georgia Cancer Center, Augusta University, Augusta, GA, USA

### Abstract

**Purpose**—Cell cycle checkpoints and DNA repair are important for cell survival after exogenous DNA damage. Both rapid blockage of G2 to M phase transition in the cell cycle and the maintenance of relatively slow G2 arrest are critical in order to protect cells from lethal ionizing radiation (IR). Checkpoint kinase 1 (CHK1) is pivotal in blocking the transition from G2 to M phases in response to IR. The 14–3–3 $\sigma$  protein is important for IR-induced G2 arrest maintenance in which p53-dependent 14–3–3 $\sigma$  transcription is involved. It has been demonstrated that Ring finger protein 126 (RNF126), an E3 ligase, is required to upregulate CHK1 expression. Thus, our goal was to study the role of RNF126 in the G2/M phase checkpoint.

**Methods and Materials**—The transition from G2 to M phases and G2 accumulation in response to IR were determined by flow cytometry through staining with phospho-histone H3 (pS10) antibody and propidium iodide, respectively. The interaction of RNF126 and 14–3–3 $\sigma$  was determined by GST-pulldown and co-immunoprecipitation (co-IP) assays. The stability of RNF126 and 14–3–3 $\sigma$  was determined by cycloheximide (CHX) based stability assay and ubiquitination detection by co-IP. The sequestering of CDK1 and cyclin B1 from the nucleus was determined by immunofluorescence staining.

**Results**—RNF126 knockdown had no impact on the IR-induced transient blockage of G2 to M but impaired IR-induced G2 arrest maintenance in cells with or without wild-type p53. Mechanistically, RNF126 binds 14–3–3 $\sigma$  and prevents both proteins from ubiquitination-mediated degradation. Last, RNF126 is required for enforcing the cytoplasmic sequestration of cyclin B1 and CDK1 proteins in response to IR.

\*Corresponding author: Junran Zhang, junran.zhang@osumc.edu.

Conflict of interest

The authors declare that they have no conflicts of interest with the contents of this article.

**Publisher's Disclaimer:** This is a PDF file of an unedited manuscript that has been accepted for publication. As a service to our customers we are providing this early version of the manuscript. The manuscript will undergo copyediting, typesetting, and review of the resulting proof before it is published in its final form. Please note that during the production process errors may be discovered which could affect the content, and all legal disclaimers that apply to the journal pertain.

**Conclusions**—RNF126 promotes G2 arrest via interaction with 14–3–3 $\sigma$ , in response to IR. Our study revealed a novel role for RNF126 in promoting G2 arrest, providing a new target for cancer treatment.

---

## Introduction

Cells respond to interference in replication and DNA damage through the activation of signal transduction pathways, more commonly known as checkpoints, in order to stop progression of the cell cycle and to promote DNA repair<sup>1</sup>. Such pathways lead to accuracy in DNA replication and chromosome segregation. However, defective checkpoint responses can lead to genome instability and even cell death<sup>2</sup>. Thus, a favorable strategy in cancer treatment is to target the proteins required for cell-cycle checkpoints.

Progression from the G2 phase to mitosis is regulated by a complex network of proteins. Direct activation of the cyclin B1/ cyclin-dependent kinase 1 (CDK1) complex and downregulation of its inhibitors control entry into mitosis<sup>3,4</sup>. The cell cycle can be interrupted by exogenous DNA damage, which includes DNA double-strand breaks (DSBs) caused by ionization radiation (IR). When DNA damage occurs during the G2 phase, a signaling cascade pathway controlling mitotic entry via regulation of cyclin B1/CDK1 complex is activated<sup>5,6</sup>. This allows cells to repair DNA damage. Thus, the G<sub>2</sub>-M DNA damage checkpoint in eukaryotic cells ensures that mitosis is not initiated until the repair of damaged or incompletely replicated DNA is complete.

Two signaling cascades are important for G2/M checkpoints. Cellular progression from G2 into mitosis is inhibited rapidly by the first cascade and can be detected by the staining of phospho-histone H3 (pS10)<sup>7</sup>. G2 arrest maintenance is the second slower cascade, which can be measured by propidium iodide staining and lasts for several hours after IR<sup>8</sup>. In response to DNA damage, CHK1, a serine/threonine-specific protein kinase, becomes activated<sup>9,10</sup> to prevent the activation of CDK1 and transiently inhibit mitotic entry from G2 phase<sup>11,12</sup>. In addition, 14–3–3 $\sigma$  plays a major role in the maintenance of G2 arrest in response to DNA damage and is mostly regulated by p53 in response to DNA damage<sup>13</sup>.

RNF126 is an E3 ubiquitin ligase that shows high expression in invasive breast and ovarian cancers and acts as an indicator of a poor prognosis<sup>14,15</sup>. RNF126, by targeting various proteins for degradation, has broad functions during cancer development<sup>16–21</sup>. Recently, a study suggested that RNF126 promotes the expression of CHK1<sup>14</sup>. Thus, we want to determine whether RNF126 plays a role in the DNA damage-induced G2/M checkpoint.

Surprisingly, we found that RNF126 has no effect on the IR-induced transient blockage of G2 to M phases but promotes IR-induced G2 accumulation in cells, with or without wild-type p53. RNF126 regulates G2 arrest by directly binding 14–3–3 $\sigma$  via region “e” of RNF126 from aa130–140<sup>21</sup>. Most importantly, IR exposure induced RNF126 and 14–3–3 $\sigma$  protein stabilization via prevention of the degradation of these two proteins. Lastly, RNF126 depletion increased the proportion of cells with nuclear CDK1 and cyclin B1 staining. Taken together, we identified a novel IR-induced G2 arrest pathway that depends on the RNF126-mediated stabilization of 14–3–3 $\sigma$ .

## Methods and Materials

### Cell lines, plasmids, transfections, and inhibitors

MCF7, MDA-MB-231, SK-BR-3, and HEK293T cells were grown in Dulbecco's Modified Eagle Medium (DMEM; Hyclone, Logan, UT, USA). HCC1143 cells were grown in Roswell Park Memorial Institute (RPMI)-1640 medium (Hyclone) with the addition of 10% bovine growth serum (Hyclone) in 5% CO<sub>2</sub> with humidity at 37°C. RNF126 and 14-3-3 $\sigma$  short hairpin RNAs (shRNAs) were supplied by Sigma-Aldrich (St Louis, MO, USA). Flag-RNF126 wild type (WT) has been described in a recent study<sup>18</sup>. His-14-3-3 $\sigma$  was obtained from Professor Haiyan Fu (Department of Pharmacology, Emory University, Atlanta, GA, USA). Lipofectamine 2000 (Invitrogen, Waltham, MA, USA) was used for DNA-plasmid transfections performed in accordance with manufacturer's suggestions. A Ni-NTA Superflow Cartridge (Cat. 30721; Qiagen, Hilden, Germany) was used to generate purified His-14-3-3 $\sigma$  protein.

### Real-time quantitative reverse transcription PCR

We performed real-time quantitative reverse transcription-PCR (qRT-PCR) as outlined before<sup>22</sup>. Primers are shown in the Supplementary Material.

### Flow cytometry

Flow cytometry assay was conducted as previously reported<sup>14</sup>. After fixation in ethanol, cells were dually stained using propidium iodide (PI) and an anti-phospho-histone H3 (pS10) specific antibody with an Alexa Fluor 488 label (Cell Signaling Technology, Danvers, MA, USA).

### Cycloheximide assay

A cycloheximide assay was performed as previously described<sup>23</sup>.

### Antibodies

To detect proteins, antibodies were used as follows: anti-RNF126 (Santa Cruz Biotechnology, Dallas TX USA, clone C-1, 1:200); anti-14-3-3 $\sigma$  (Santa Cruz Biotechnology, clone C-18, 1:200); anti-FLAG (Sigma-Aldrich, clone M2, 1:1000); anti-GST (Santa Cruz Biotechnology, 1-109, 1:200), anti- $\beta$ -actin (Sigma-Aldrich, clone AC-74, 1:50000); anti-His (Santa Cruz Biotechnology, Clone H-15, 1:200); and anti-phospho-histone H3-Ser10 (Cell Signaling Technology, #3377S). Cell Signaling Technology's goat anti-mouse IgG-horseradish peroxidase (HRP) (#7076S, 1:1000) and goat anti-rabbit IgG-HRP (#7074S, 1:1000) were subsequently used as secondary antibodies. The primary antibodies used for immunofluorescence were anti-CDK1 (Abcam, ab133327, 1:100), and anti-cyclin B1 (Santa Cruz Biotechnology, sc-245, 1:100). Thermo Fisher Scientific's goat anti-mouse IgG (H+L) Alexa Fluor 594 (A-11032, 1:400), and chicken anti-rabbit IgG (H+L) Alexa Fluor 488 (A-21441, 1:400) were used as secondary antibodies.

### Radiation sources

Cesium-137 gamma rays were used at a dose rate of 3.1 Gray/min to irradiate cells.

### Ubiquitination assay

Ubiquitination was detected after transiently co-transfecting cells with the indicated plasmids. After incubating for 48 h, 5  $\mu$ M MG132 was added to cells for 6 h. Ubiquitinated proteins were immunoprecipitated by antibodies as indicated.

### GST fusion proteins and pull-down assay

A glutathione S-transferase (GST) pull-down assay was performed according to a recent study <sup>22</sup>.

### Immunoprecipitation and immunoblotting

Cellular samples were immunoprecipitated, electrophoresed and then immunoblotted as described in a recent study <sup>24</sup>.

### Immunofluorescence assays

Immunofluorescence assays were performed as described in a recent study <sup>23</sup>.

## Results

### 1. RNF126 is required for G2 arrest without affecting the rapid transition from G2 to M phases in response to IR

Given that RNF126 can regulate CHK1 protein expression <sup>14</sup>, we wanted to determine whether RNF126 affects the G2/M checkpoint. We first measured the effect of RNF126 on IR-induced blockage of a transient transition from a G2 to M phase by analyzing phosphor-histone H3-Ser10 staining, which is widely used to show cells in the M phase. In our study, both p53 wild-type (MCF7) and mutant (MDA-MB-231) cell lines were used. In control cells, IR exposure induced a dramatic decrease in the percentage of M phase cells, indicating an effective G2/M phase checkpoint that blocked the progression of G2 to M phase following IR exposure. Surprisingly, a similar pattern was observed in cells depleted of RNF126, indicating RNF126 is not necessary in the IR-induced blockage of the G2-M transition, regardless of p53 expression status (Fig. 1A). We found similar results in MDA-MB-231 and MCF7 cells using a second shRNA of RNF126 (Fig. S1A). We next determined G2/M accumulation at different time points of IR (up to 8 h post-IR) using PI staining. Interestingly, RNF126 depletion reduced IR-induced G2/M accumulation, compared to cells with intact RNF126, indicating that RNF126 depletion abolished IR-induced G2/M arrest (Fig. 1B). The second RNF126 shRNA yielded a similar result (Fig. S1B). Since RNF126 depletion did not affect the percentage of cells with mitotic entry, RNF126 depletion that abrogated the IR-induced increase in the portion of G2/M phase cells could be due to a reduced cell number in the G2 phase. Thus, RNF126 is necessary for maintaining G2 arrest in cells with or without wild-type p53.

It has been suggested that G2 arrest occurs at much later times after IR ( 24 h, post-IR) and most likely represents the accumulation of cells that have been in earlier phases of the cell cycle at the time of exposure to radiation. In addition, Ataxia-telangiectasia mutated ( ATM) inhibition can enhance G2 arrest ( 24 h, post-IR) <sup>8</sup>. Thus, we next determined G2 arrest in the extended hours after IR in both MCF7 and MDA-MB-231 cells, two cell lines with

a different ability in arresting cells in the earlier phase of the cell cycle when challenged with DNA damaging agents. It has been demonstrated that an arrest of earlier S and/or G1/S phases occurs in MCF7 cells after treatment with DNA damaging agents<sup>25,26</sup>, suggesting that the earlier phase of the cell cycle might have a minimal impact in G2 accumulation in response to DNA damage because cells arrest in the earlier phase of the cell cycle. In contrast, MDA-MB-231 cells cannot block cells in the G1/S phase in response to DNA damage and are still able to move to the G2/M phase when challenged with DNA damaging agents. Thus, the earlier cell-cycle phase affected G2 arrest. Our study suggests that RNF126 knockdown impaired G2 arrest at <24 h post-IR in both cell lines (Fig. 1, Fig. S2). However, the G2 arrest at <24 h post-IR may be different to the G2 arrest that occurs much later (24h, post-IR) due to the following reasons: In support of the result from a previous report that ATM inhibition enhances G2 arrest in later hours (24 h, post-IR)<sup>8</sup>, ATM inhibition indeed enhanced G2 arrest in MDA-MB-231 cells (24 h, post-IR). However, in our study, RNF126 knockdown had no impact on G2 arrest at later time points (24 h, post-IR) in MCF7 cells (Fig. S2B). As a control, the IR-induced blockage of a transient transition from a G2 to M phase was monitored by analyzing phosphor-histone H3-Ser10 staining (Fig. S2C). Therefore, it is most likely that G2 arrest detected <24 h post-IR might be different to that are detected in later hours (24 h, post-IR). RNF126 knockdown impaired G2 arrest (<24 h) in cells, with or without ATM inhibition (Fig. S2).

## 2. RNF126 binds to 14–3–3 $\sigma$ through aa130–140 (region “e”) and the association of these two proteins is increased in response to IR

RNF126 and Breast Cancer Associated gene 2 (BCA2) share 46% of overall amino acids, and show 75% identity in RING domains. Consensus 14–3–3-binding sites (311–555 b for RNF126) are encoded by both genes<sup>27</sup>. A direct interaction between BCA2 and 14–3–3 $\sigma$  has been identified<sup>28</sup>. Because of the activity of 14–3–3 $\sigma$  in G2 arrest, a co-IP assay was used to examine the association between RNF126 and 14–3–3 $\sigma$ . Flag-RNF126-WT and His-14–3–3 $\sigma$  were overexpressed in MCF7 cells. Immunoprecipitation of RNF126 was conducted with an anti-Flag antibody, and exogenous His-14–3–3 $\sigma$  was found in an anti-Flag associated protein complex (Fig. 2A). Additionally, binding between endogenous RNF126 and 14–3–3 $\sigma$  proteins was also detected in MCF7 as well as MDA-MB-231 cells using both anti-14–3–3 $\sigma$  (Fig. 2B) and RNF126 (Fig. S3A) antibodies. Thus, RNF126 and 14–3–3 $\sigma$  proteins are shown to interact in a physiological setting. To determine whether RNF126 can directly interact with 14–3–3 $\sigma$ , a GST pull-down assay was conducted. We purified recombinant GST-RNF126-WT and His-14–3–3 $\sigma$  proteins. The result suggested a direct interaction between RNF126 and 14–3–3 $\sigma$  (Fig. 2C). The “e” region of RNF126 from 130aa to 140aa is located within a region that potentially interacts with 14–3–3 $\sigma$  (Fig. 2D)<sup>27</sup>. We thus determined whether the “e” region of RNF126 was required for the interaction of these two proteins. GST-RNF126-WT and GST-RNF126-e proteins were purified *in vitro* and then incubated with cell lysates prepared from MCF7 cells transfected with His-14–3–3 $\sigma$ -expressing plasmid. The result suggested that GST-RNF126-WT interacted with 14–3–3 $\sigma$ ; however, the association between GST-RNF126-e and 14–3–3 $\sigma$  was significantly reduced (Fig. 2E). This result was further verified using purified His-14–3–3 $\sigma$  protein. GST-RNF126-WT directly interacted with 14–3–3 $\sigma$  whereas GST-RNF126-e impaired their interaction

(Fig. 2F). Thus, our results suggest a direct interaction occurs between RNF126 and 14-3-3 $\sigma$ , with the “e” region of RNF126 important for the association of these two proteins.

Next, we examined the association between these two proteins in response to IR. We determined whether the RNF126 and 14-3-3 $\sigma$  interaction is increased using a co-IP assay. Flag-RNF126-WT- and His-14-3-3 $\sigma$ -expressing plasmids were transfected into HEK293T cells (Fig. 2G). The amount of 14-3-3 $\sigma$  that was associated with RNF126 increased after IR since His-tagged 14-3-3 $\sigma$  protein detected in anti-Flag immunoprecipitation complexes was increased in irradiated cells in comparison to unirradiated cells. We next determined the IR-induced association of endogenous RNF126 and 14-3-3 $\sigma$  proteins by co-IP. Consistently, the reciprocal endogenous interaction between RNF126 and 14-3-3 $\sigma$  was increased in response to IR in MCF7 (Fig. 2H) and MDA-MB-231 (Fig. S3B) cells. Additionally, we also determined whether expression of Flag-RNF126- e led to a decrease in the IR-induced association of RNF126 with 14-3-3 $\sigma$ . An immunoprecipitation assay was undertaken using cell lysate prepared from MCF7 and MDA-MB-231 cells expressing Flag-RNF126-WT or Flag-RNF126- e. In brief, cells were co-transfected with His-14-3-3 $\sigma$  and Flag-RNF126-WT or Flag-RNF126- e. His-14-3-3 $\sigma$  and endogenous 14-3-3 $\sigma$  were detected in anti-Flag-RNF126-WT immunoprecipitates, especially in cells treated with IR. However, reduced levels of His-14-3-3 $\sigma$  and endogenous 14-3-3 $\sigma$  proteins were detected in anti-Flag-RNF126- e immunoprecipitates. A similar amount of Flag-RNF126-WT and Flag-RNF126- e was immunoprecipitated (Fig. 2I). In the same setting, Flag-RNF126-WT was detected in anti-His or anti-14-3-3 $\sigma$  immunoprecipitates, especially in the cells treated with IR but a much less Flag-RNF126- e was detected (Fig.S3C). Lastly, the RNF126- e expression reduced the association with 14-3-3 $\sigma$  in the HEK293T cells (Fig. S3D). Thus, our results suggest that the association of RNF126 and 14-3-3 $\sigma$  increased upon IR in both p53 wild-type and mutant cells and the region “e” of RNF126 is important for the association of RNF126 and 14-3-3 $\sigma$ .

### 3. IR-induced 14-3-3 $\sigma$ protein expression depends on RNF126

14-3-3 $\sigma$  protein expression increased in response to IR<sup>29</sup>. Given the direct interaction of RNF126 and 14-3-3 $\sigma$  (Fig. 2), we next determined whether RNF126 was important for IR-induced 14-3-3 $\sigma$  protein expression. First, we measured the 14-3-3 $\sigma$  protein level in MCF7 and MDA-MB-231 cells and found that it increased after IR (Fig. 3A). Two additional p53 mutant cell lines showed similar results. RNF126 knockdown impaired G2 arrest, which is associated with increased 14-3-3 $\sigma$  protein levels (Fig. S4A). Impaired G2 arrest was also found in such cells (<24 h, post-IR; Fig. S4B, C). However, IR only induced 14-3-3 $\sigma$  transcript expression in MCF7 but not MDA-MB-231 cells (Fig. 3B), as found in a previous report, suggesting that IR induces an increase in 14-3-3 $\sigma$  transcript in cells with wild-type p53<sup>30</sup>. We next determined how RNF126 depletion affected IR-induced 14-3-3 $\sigma$  expression. 14-3-3 $\sigma$  expression induced by IR in both MCF7 and MDA-MB-231 cells was abrogated when RNF126 was downregulated using two different shRNAs (Fig. 3C). However, this effect was not associated with transcriptional regulation since an identical level of 14-3-3 $\sigma$  transcripts was found, with or without RNF126 knockdown, in MCF7 as well as MDA-MB-231 cell lines (Fig. 3D). Thus, Fig. 3 suggests that RNF126 is necessary for IR-induced 14-3-3 $\sigma$  protein expression, even in cells with mutant p53.

#### 4. RNF126 is required for 14–3–3 $\sigma$ protein stability in response to IR

RNF126 is an E3 ligase. To determine whether RNF126 with defective E3 ligase function is involved in the regulation of 14–3–3 $\sigma$  protein expression, wild-type RNF126 and RNF126 E3 ligase mutant (Flag-RNF126-C229A/-C232A) plasmids were overexpressed in MCF7 and MDA-MB-231 cells. 14–3–3 $\sigma$  protein increased in both RNF126 E3 ligase mutant and wild-type RNF126-expressing cells (Fig. 4A). This indicated that the loss of E3 ligase function does not interfere with 14–3–3 $\sigma$  protein expression. We next measured the effect of RNF126 on the half-life of 14–3–3 $\sigma$  protein by CHX assay in MCF7 cells. We found that RNF126 depletion reduced the half-life of 14–3–3 $\sigma$  protein (Fig. 4B). This suggested that RNF126 might prevent the degradation of 14–3–3 $\sigma$  protein. Furthermore, we found that the prevention of 14–3–3 $\sigma$  degradation by RNF126 requires interaction between these two proteins, since the expression of RNF126- e failed to cause increased 14–3–3 $\sigma$  protein expression (Fig. 4C). Therefore, although RNF126 is an E3 ligase, RNF126 overexpression led to increased 14–3–3 $\sigma$  protein expression independent of its E3 ligase activity. This also supports the hypothesis that RNF126 stabilizes 14–3–3 $\sigma$  as a result of the direct interaction of these two proteins. Therefore, we next observed the impact of expression of RNF126- e on IR-induced 14–3–3 $\sigma$  protein expression. Flag-RNF126-WT overexpression led to increased 14–3–3 $\sigma$  protein expression. However, IR-induced 14–3–3 $\sigma$  protein was abrogated in cells expressing Flag-RNF126- e (Fig. 4D). We next determined the 14–3–3 $\sigma$  ubiquitination level in cells with or without RNF126 depletion, in MCF7 and also MDA-MB-231 cells. As anticipated, RNF126 deficiency increased the ubiquitination level of 14–3–3 $\sigma$ , especially in irradiated cells (Fig. 4E). Thus, our results suggest that RNF126 is important for 14–3–3 $\sigma$  stability in response to IR by preventing its ubiquitination-dependent degradation.

#### 5. IR-induced RNF126 is stabilized by binding 14–3–3 $\sigma$

A previous report showed that BCA2, which shares a similar protein structure with RNF126, is stabilized by substrate interactions with 14–3–3 $\sigma$ <sup>28</sup>. Since IR induced both RNF126 and 14–3–3 $\sigma$  expression simultaneously (Fig. 3A and Fig. 5A), and IR-induced 14–3–3 $\sigma$  protein expression depends on RNF126 (Fig. 3), we hypothesize that 14–3–3 $\sigma$  promotes RNF126 stability as well. Indeed, 14–3–3 $\sigma$  knockdown leads to decreased RNF126 protein expression, which correlated with a decreased half-life and increased RNF126 ubiquitination (Fig. 5B–D). Therefore, it is possible that the stability of RNF126 is also dependent on 14–3–3 $\sigma$ . The region “e” of RNF126 is critical for RNF126 protein stability<sup>21</sup>. Next, we measured levels of Flag-RNF126- e protein after treating cells with a proteasome inhibitor, MG132. Equal amounts of Flag-RNF126-WT and Flag-RNF126- e plasmids were co-expressed in MCF7 cells. Lysates were collected after treating cells with or without MG132. In the presence of MG132, Flag-RNF126- e protein expression was restored to the levels of Flag-RNF126-WT (Fig. 5E, lower panel). In contrast, mRNA levels of Flag-RNF126- e were similar to those of Flag-RNF126-WT (Fig. 5E, upper panel), indicating that low expression of Flag-RNF126- e is not due to regulation at the mRNA level; RNF126- e protein was degraded via proteasome-dependent mechanisms. We next determined the RNF126 ubiquitination level. MCF7 cells co-expressing HA-Ub plasmids and Flag-RNF126-WT or Flag-RNF126- e were treated with MG132, or dimethyl sulfoxide control. Cell lysates were coimmunoprecipitated with Flag antibody, and the RNF126

ubiquitination level was detected using HA antibody. The ubiquitin level of RNF126 was lower compared to cells expressing RNF126- e, especially in cells treated with IR (Fig. 5F). Given the “e” region is important for the binding of RNF126 to 14-3-3 $\sigma$ , stabilization of RNF126 might depend on binding to 14-3-3 $\sigma$ . In support of the result showing that 14-3-3 $\sigma$  is also necessary for IR-induced RNF126 protein stability, the increase in IR-induced RNF126 protein expression was abrogated in cells depleted of 14-3-3 $\sigma$  by two different shRNAs (Fig. 5G). However, depletion of 14-3-3 $\sigma$  had no effect on the RNF126 mRNA level in MCF7 as well as MDA-MB-231 cells, indicating that 14-3-3 $\sigma$  regulates RNF126 protein stability but not RNF126 transcripts (Fig. 5H). Therefore, collectively, our results suggest that 14-3-3 $\sigma$  also, in turn, protects RNF126 from ubiquitination-dependent degradation.

## 6. RNF126 is required for sequestering CDK1 and cyclin B1 from the nucleus

As one of the key protein kinases for G2/M transition, CDK1 binds to and is activated by its activating partner, cyclin B1<sup>11</sup>. Given that 14-3-3 $\sigma$  regulates G2 arrest via sequestration of CDK1/cyclin B1, we next determined how the RNF126 status regulates the localization of CDK1/cyclin B1. By immunostaining, we evaluated the localization of CDK1/cyclin B1 in MCF7 cells with or without RNF126 depletion. Prior to IR, the knockdown of RNF126 caused the nuclear import of a small amount of CDK1/cyclin B1. However, the amount of CDK1/cyclin B1 nuclear staining was dramatically higher in cells with an RNF126 deficiency in response to IR at 4 h post-IR (Fig. 6A, B). In addition, region “e” is necessary for the sequestration of CDK1/cyclin B1, since overexpression of Flag-RNF126- e also led to the increased nuclear import of CDK1/cyclin B1. However, cells overexpressing Flag-RNF126-WT caused the decreased nuclear import of CDK1/cyclin B1 (Fig. 6C and Fig. S5). Moreover, the same results were also found in MDA-MB-231 cells (Fig. S6 and Fig. S7). Together, our results suggest that RNF126 is required for the IR-induced nuclear import of CDK1/cyclin B1 in cells with or without wild-type p53, which is consistent with its role in the maintenance of G2 arrest.

## Discussion

DNA damage-induced cell-cycle checkpoints protect cells from the lethal effects of IR. Elucidating the mechanisms involved in cell-cycle regulation might uncover new molecular targets for cancer therapy, especially for radiotherapy. Our study identified a novel role for RNF126 in DNA damage-induced G2 arrest via regulation of 14-3-3 $\sigma$  protein stability. In addition, our study discovered a novel mechanism governing G2 arrest in which the interaction of RNF126 and 14-3-3 $\sigma$  is required.

Although RNF126 regulates CHK1 expression<sup>14</sup>, our study suggests that RNF126 has no role in the transient movement of G2 to M phase in response to IR (Fig. 1); this may be due to compensation by CHK2. CHK1 is thought to respond mostly to single-strand breaks, which are created during the collapse of replication forks. However, the major kinase that responds to DSBs is thought to be CHK2<sup>31-33</sup>. Therefore, CHK2 could compensate for the defect in blockage of G2 to M transition<sup>34</sup>. In addition, it is also likely that reduced CHK1 expression in cells with RNF126 downregulation is still sufficient to function in

G2/M checkpoints. Of note, it has been suggested that the radiation-induced phosphorylation of CHK1 was associated with CHK1 binding to 14-3-3 $\sigma$ <sup>35</sup>. Thus, we cannot exclude the possibility that the role of RNF126 in G2 arrest and CDK1 translocation is also associated with CHK1 activity.

The 14-3-3 family constitutes a conserved class of seven isoforms and takes part in many cellular processes<sup>36-38</sup>. In the presence of DNA damage, CDK1 is activated through dephosphorylation by the CDC25 phosphatase family<sup>39</sup>. Various 14-3-3 isoforms are important for DNA damage-induced G2/M checkpoints by binding to CDC25 proteins<sup>40,41</sup>. For instance, 14-3-3 proteins reduce CDC25 activity in *Xenopus* via direct binding<sup>42</sup>. 14-3-3 $\beta$  binding to CDC25B leads to imperfect nuclear import that causes the majority of CDC25B to relocalize to the cytoplasm. This leads to the exclusion of CDC25 from the nucleus or its sequestration in the cytoplasm and, in turn, fails to activate the CDK1/cyclin B complex. However, this does not occur for 14-3-3 $\sigma$ <sup>43</sup>. In contrast, 14-3-3 $\sigma$  promotes G2 arrest by enforcing sequestration of the CDK1/cyclin B complex<sup>44</sup>. It has been demonstrated that the CDK1/cyclin B complex is important to DNA damage-induced G2/M checkpoint activation, which requires the transcriptional induction of 14-3-3 $\sigma$  via p53. Hermeking et al. also found IR led to the upregulation of 14-3-3 $\sigma$  by p53, allowing DNA damaged cells to be retained in a G2-arrested state, functioning in parallel with p21<sup>30,45,46</sup>. Here, we provide strong evidence suggesting that RNF126 has a novel role in promoting G2 arrest. Therefore, we reveal an unrecognized mechanism that promotes G2 arrest, in which the direct binding of RNF126 and 14-3-3 $\sigma$  is required. We hypothesize that the association and stabilization of RNF126 and 14-3-3- $\sigma$  is required for G2 arrest. However, the mechanisms by which protein stabilization occur remain unknown. The interaction of these two proteins can interrupt ubiquitination-mediated degradation. It has been suggested that 14-3-3 $\sigma$  affects the auto-ubiquitination and auto-degradation activity of BCA2, a close relative of RNF126<sup>28</sup>. It would be very interesting to determine whether 14-3-3 $\sigma$  affects RNF126 stability by suppressing RNF126 self-ubiquitination. Of note, although our study suggested a role for RNF126 in the maintenance of G2 arrest in the cells, with or without wild type p53, we cannot exclude the involvement of p53 since MCF7 and MDA-231 cells are not isogenic paired cell lines. Additionally, a recent study has demonstrated that RNF126 promotes homologous recombination repair that relies on its interaction with the transcriptional regulator, E2F1. However, this regulation is independent of E3 ligase activity<sup>14</sup>. This study has yielded evidence to support a novel function of RNF126 in the maintenance of G2 arrest that is not based on its E3 ligase activity. Therefore, the results reported in this study as well as in our prior work suggest that E3 ligase protein can function using an E3 ligase-independent mechanism.

Our discoveries raise two intriguing questions. First, given 14-3-3 are phosphorylation binding proteins, it would be of interest to know if IR can induce the phosphorylation of RNF126. Second, further research is required to clarify how the direct binding of RNF126 and 14-3-3 $\sigma$  prevents the degradation of RNF126. This is a common mechanism by which protein-protein interaction blocks the accessibility of E3 ligase to target proteins, leading to stabilization. However, this needs to be tested in the future.

Based on the experimental data described above, our study has established a novel role for RNF126 in promoting G2 arrest via interaction with 14–3–3 $\sigma$ . This suggests that even in p53-defective tumor cells, the RNF126/14–3–3 $\sigma$  pathway can still mediate G2 arrest, highlighting its usefulness as a therapeutic target.

## Supplementary Material

Refer to Web version on PubMed Central for supplementary material.

## Acknowledgements

Our thanks go to Shared Resource at The Ohio State University Comprehensive Cancer Center for the service provided by The Flow Cytometry Shared Resource (FCSR).

Funding and additional information

The following grants, in part, supported this work: NIH/NCI R01CA240374, and R01CA249198; and Awards from Department of Defense (Congressionally Directed Medical Research Programs and from the Breast Cancer Alliance and from the Case Comprehensive Cancer Center (VeloSano Bike to Cure) and from the Ohio State University James Comprehensive Cancer Intramural Research Program (Pelotonia) (to J. Zhang). Financial support was also forthcoming from The Ohio State University Comprehensive Cancer Center and the National Institutes of Health under grant number P30 CA016058.

## Data Availability

Research data are stored in an institutional repository and will be shared upon request to the corresponding author.

## References

1. Lukas J, Lukas C, Bartek J. Mammalian cell cycle checkpoints: signalling pathways and their organization in space and time. *DNA Repair (Amst)*. 2004;3(8–9):997–1007. [PubMed: 15279786]
2. Kaufmann WK, Nevis KR, Qu P, et al. Defective cell cycle checkpoint functions in melanoma are associated with altered patterns of gene expression. *J Invest Dermatol*. 2008;128(1):175–187. [PubMed: 17597816]
3. Mueller PR, Coleman TR, Kumagai A, Dunphy WG. Myt1-a Membrane-Associated Inhibitory Kinase That Phosphorylates Cdc2 on Both Threonine-14 and Tyrosine-15. *Science*. 1995;270(5233):86–90. [PubMed: 7569953]
4. Parker LL, Atherton-Fessler S, Piwnicka-Worms H. p107wee1 is a dual-specificity kinase that phosphorylates p34cdc2 on tyrosine 15. *Proceedings of the National Academy of Sciences of the United States of America*. 1992;89(7):2917–2921. [PubMed: 1372994]
5. Gavet O, Pines J. Progressive activation of CyclinB1-Cdk1 coordinates entry to mitosis. *Dev Cell*. 2010;18(4):533–543. [PubMed: 20412769]
6. Pines J, Hunter T. Human cyclin A is adenovirus E1A-associated protein p60 and behaves differently from cyclin B. *Nature*. 1990;346(6286):760–763. [PubMed: 2143810]
7. Wei Y, Mizzen CA, Cook RG, Gorovsky MA, Allis CD. Phosphorylation of histone H3 at serine 10 is correlated with chromosome condensation during mitosis and meiosis in *Tetrahymena*. *Proceedings of the National Academy of Sciences of the United States of America*. 1998;95(13):7480–7484. [PubMed: 9636175]
8. Xu B, Kim ST, Lim DS, Kastan MB. Two Molecularly Distinct G2/M Checkpoints Are Induced by Ionizing Irradiation. *Molecular and Cellular Biology*. 2002;22(4):1049–1059. [PubMed: 11809797]
9. Wolkow TD, Enoch T. Fission yeast Rad26 is a regulatory subunit of the Rad3 checkpoint kinase. *Molecular biology of the cell*. 2002;13(2):480–492. [PubMed: 11854406]

10. Verkade HM, Bugg SJ, Lindsay HD, Carr AM, O'Connell MJ. Rad18 is required for DNA repair and checkpoint responses in fission yeast. *Molecular biology of the cell*. 1999;10(9):2905–2918. [PubMed: 10473635]
11. Chow JP, Poon RY, Ma HT. Inhibitory phosphorylation of cyclin-dependent kinase 1 as a compensatory mechanism for mitosis exit. *Mol Cell Biol*. 2011;31(7):1478–1491. [PubMed: 21262764]
12. Gatei M, Sloper K, Sørensen C, et al. Ataxia-telangiectasia-mutated (ATM) and NBS1-dependent Phosphorylation of Chk1 on Ser-317 in Response to Ionizing Radiation\*. *Journal of Biological Chemistry*. 2003;278(17):14806–14811.
13. Chan TA, Hermeking H, Lengauer C, Kinzler KW, Vogelstein B. 14–3–3Sigma is required to prevent mitotic catastrophe after DNA damage. *Nature*. 1999;401(6753):616–620. [PubMed: 10524633]
14. Yang X, Pan Y, Qiu Z, et al. RNF126 as a biomarker of a poor prognosis in invasive breast cancer and CHEK1 inhibitor efficacy in breast cancer cells. *Clin Cancer Res* 2018;24:1629–1643. [PubMed: 29326282]
15. Wang C, Wen A, Qiao J, Liu Y, Guo Y, Wang W. High Expression of RING Finger Protein 126 Predicts Unfavorable Prognosis of Epithelial Ovarian Cancer. *Med Sci Monit*. 2020;26:e921370. [PubMed: 32254065]
16. Smith CJ, Berry DM, McGlade CJ. The E3 ubiquitin ligase RNF126 in breast cancer. *Neoplasia* 2006;8:689–695. ligases RNF126 and Rabr17 regulate endosomal sorting of the epidermal growth factor receptor. *Journal of cell science*. 2013;126(Pt 6):1366–1380. [PubMed: 23418353]
17. Kamikubo K, Kato H, Kioka H, et al. A molecular triage process mediated by RING finger protein 126 and BCL2-associated athanogene 6 regulates degradation of G0/G1 switch gene 2. *The Journal of biological chemistry*. 2019;294(40):14562–14573. [PubMed: 31371451]
18. Zhi X, Zhao D, Wang Z, et al. E3 ubiquitin ligase RNF126 promotes cancer cell proliferation by targeting the tumor suppressor p21 for ubiquitin-mediated degradation. *Cancer research*. 2013;73(1):385–394. [PubMed: 23026136]
19. Hu X, Wang L, Wang Y, et al. RNF126-Mediated Reubiquitination Is Required for Proteasomal Degradation of p97-Extracted Membrane Proteins. *Molecular cell*. 2020;79(2):320–331 e329. [PubMed: 32645369]
20. Ishida N, Nakagawa T, Iemura SI, et al. Ubiquitylation of Ku80 by RNF126 Promotes Completion of Nonhomologous End Joining-Mediated DNA Repair. *Mol Cell Biol*. 2017;37(4).
21. Wang Y, Deng O, Feng Z, et al. RNF126 promotes homologous recombination via regulation of E2F1-mediated BRCA1 expression. *Oncogene* 2016;35:1363–1372. [PubMed: 26234677]
22. Zhang J, Ma Z, Treszezamsky A, Powell SN. MDC1 interacts with Rad51 and facilitates homologous recombination. *Nat Struct Mol Biol* 2005;12:902–909. [PubMed: 16186822]
23. Qiu Z, Fa P, Liu T, et al. A Genome-Wide Pooled shRNA Screen Identifies PPP2R2A as a Predictive Biomarker for the Response to ATR and CHK1 Inhibitors. *Cancer research* 2020;80:3305–3318. [PubMed: 32522823]
24. Feng Z, Zhang J. A dual role of BRCA1 in two distinct homologous recombination mediated repair in response to replication arrest. *Nucleic Acids Res* 2012;40:726–738. [PubMed: 21954437]
25. Bar-On O, Shapira M, Hershko DD. Differential effects of doxorubicin treatment on cell cycle arrest and Skp2 expression in breast cancer cells. *Anticancer Drugs* 2007;18:1113–1121. ra M, Hershko DD. Differential effects of doxorubicin treatment on cell cycle arrest and Skp2 expression in breast cancer cells. *Anticancer Drugs*. 2007;18(10):1113–1121. [PubMed: 17893511]
26. Aarts M, Sharpe R, Garcia-Murillas I, et al. Forced mitotic entry of S-phase cells as a therapeutic strategy induced by inhibition of WEE1. *Cancer discovery*. 2012;2(6):524–539 [PubMed: 22628408]
27. Burger A, Amemiya Y, Kitching R, Seth AK. Novel RING E3 ubiquitin ligases in breast cancer. *Neoplasia* 2006;8:689–695. [PubMed: 16925951]
28. Bacopulos S, Amemiya Y, Yang W, et al. Effects of partner proteins on BRCA2 RING ligase activity. *BMC cancer*. 2012;12:63. [PubMed: 22315970]

29. Guweidhi A, Kleeff J, Giese N, et al. Enhanced expression of 14–3-3sigma in pancreatic cancer and its role in cell cycle regulation and apoptosis. *Carcinogenesis*. 2004;25(9):1575–1585. [PubMed: 15073049]
30. Hermeking HLC, Polyak K, He TC, Zhang L, Thiagalingam S, Kinzler KW, Vogelstein B. 14–3-3sigma is a p53-regulated inhibitor of G2/M progression. *Molecular cell*. 1997;1:3–11. [PubMed: 9659898]
31. Jazayeri A, Falck J, Lukas C, et al. ATM- and cell cycle-dependent regulation of ATR in response to DNA double-strand breaks. *Nature cell biology*. 2006;8(1):37–45. [PubMed: 16327781]
32. Suzuki K, Kodama S, Watanabe M. Recruitment of ATM Protein to Double Strand DNA Irradiated with Ionizing Radiation\*. *Journal of Biological Chemistry*. 1999;274(36):25571–25575.
33. Smith J, Tho LM, Xu N, Gillespie DA. The ATM-Chk2 and ATR-Chk1 pathways in DNA damage signaling and cancer. *Advances in cancer research*. 2010;108:73–112. [PubMed: 21034966]
34. van Jaarsveld MTM, Deng D, Ordonez-Rueda D, Paulsen M, Wiemer EAC, Zi Z. Cell-type-specific role of CHK2 in mediating DNA damage-induced G2 cell cycle arrest. *Oncogenesis*. 2020;9(3):35. [PubMed: 32170104]
35. Tian H, Faje AT, Lee SL, Jorgensen TJ. Radiation-induced phosphorylation of Chk1 at S345 is associated with p53-dependent cell cycle arrest pathways. *Neoplasia*. 2002;4(2):171–180. [PubMed: 11896572]
36. Phan L, Chou PC, Velazquez-Torres G, et al. The cell cycle regulator 14–3-3sigma opposes and reverses cancer metabolic reprogramming. *Nature communications*. 2015;6:7530.
37. Nathan KG, Lal SK. The Multifarious Role of 14–3-3 Family of Proteins in Viral Replication. *Viruses*. 2020;12(4):436.
38. Cornell B, Toyo-oka K. 14–3-3 Proteins in Brain Development: Neurogenesis, Neuronal Migration and Neuromorphogenesis. *Frontiers in Molecular Neuroscience*. 2017;10(318).
39. Timofeev O, Cizmecioglu O, Settele F, Kempf T, Hoffmann I. Cdc25 Phosphatases Are Required for Timely Assembly of CDK1-Cyclin B at the G2/M Transition\*. *Journal of Biological Chemistry*. 2010;285(22):16978–16990.
40. Lopez-Girona AFB, Mondesert O, Russell P. Nuclear localization of Cdc25 is regulated by DNA damage and a 14–3-3 protein. *Nature*. 1999;397:172–175. [PubMed: 9923681]
41. Peng CY, Graves PR, Thoma RS, Wu Z, Shaw AS, Piwnicka-Worms H. Mitotic and G2 checkpoint control: regulation of 14–3-3 protein binding by phosphorylation of Cdc25C on serine-216. *Science*. 1997;277(5331):1501–1505. [PubMed: 9278512]
42. Kumagai AYP, Dunphy WG. 14–3-3 proteins act as negative regulators of the mitotic inducer Cdc25 in *Xenopus* egg extracts. *Mol Biol Cell*. 1998;9:345–354. [PubMed: 9450960]
43. Uchida S, Kuma A, Ohtsubo M, et al. Binding of 14–3-3beta but not 14–3-3sigma controls the cytoplasmic localization of CDC25B: binding site preferences of 14–3-3 subtypes and the subcellular localization of CDC25B. *Journal of cell science*. 2004;117(14):3011–3020. [PubMed: 15173315]
44. Laronga C, Yang HY, Neal C, Lee MH. Association of the cyclin-dependent kinases and 14–3-3 sigma negatively regulates cell cycle progression. *The Journal of biological chemistry*. 2000;275(30):23106–23112. [PubMed: 10767298]
45. Rajagopalan S, Sade RS, Townsley FM, Fersht AR. Mechanistic differences in the transcriptional activation of p53 by 14–3-3 isoforms. *Nucleic Acids Res*. 2010;38(3):893–906. [PubMed: 19933256]
46. Chan TA, Hwang PM, Hermeking H, Kinzler KW, Vogelstein B. Cooperative effects of genes controlling the G(2)/M checkpoint. *Genes & development*. 2000;14(13):1584–1588. [PubMed: 10887152]

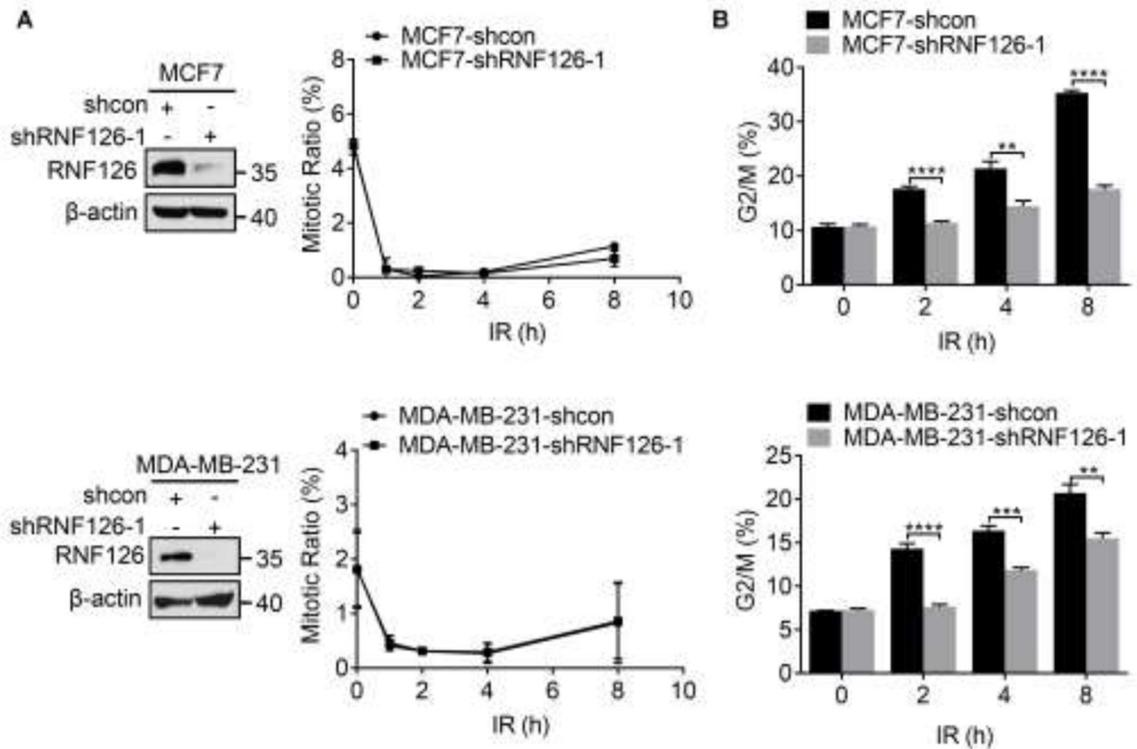


**Figure 1. RNF126 is required for G2 arrest without affecting the rapid transition from G2 to M in response to IR.**

(A) RNF126 deficiency has no effect on the mitotic ratio in MCF7 and MDA-MB-231 cells following ionizing radiation (IR; 8 Gy). Protein levels were assessed with western blotting.  $\beta$ -actin was used as a loading control (left panel). Early G2/M checkpoint data were quantitated using phosphor-histone H3-Ser10 antibody (right panel). (B) The percentage of total cells in G2/M phase after RNF126 knockdown, with or without IR (8 Gy), in both MCF7 (upper panel) and MDA-MB-231 (lower panel) cells. shRNA, short hairpin RNA.  $**P < 0.01$ ,  $***P < 0.001$ ,  $****P < 0.0001$ . All data represent the mean  $\pm$  SEM from three independent experiments. Statistical significance was determined using Student's *t* test.

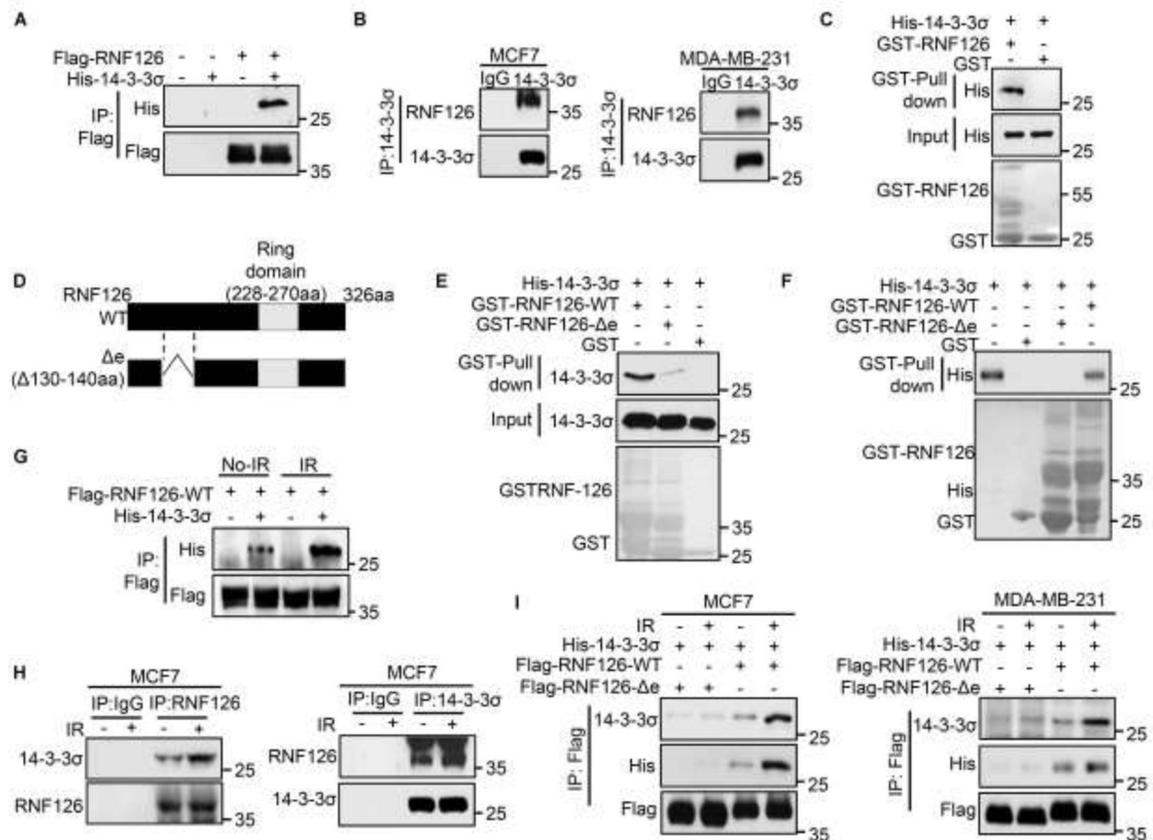


**Figure 2. RNF126 binds to 14-3-3 $\sigma$  through aa130-140 (region “e”) and the association of these two proteins is increased in response to IR.**

(A) RNF126 associates with 14-3-3 $\sigma$  in an immunoprecipitation (IP) assay. HEK293T cells were co-transfected with Flag-RNF126-wild type (WT) and His-14-3-3 $\sigma$  plasmids. Cell lysates were immunoprecipitated with Flag-specific antibody. (B) Endogenous interaction between RNF126 and 14-3-3 $\sigma$ . (C) RNF126 directly binds to 14-3-3 $\sigma$  by using a Glutathione S-transferase (GST)-pull down assay. (D) The schematic map for region “e” from 130 to 140aa in RNF126. (E, F) Region “e” of RNF126 was necessary for the association with 14-3-3 $\sigma$ . His-14-3-3 $\sigma$  plasmid was transfected into MCF7 cells (E). His-14-3-3 $\sigma$  protein was purified using a Ni-NTA Superflow Cartridge (F). Cell lysate or purified 14-3-3 $\sigma$  protein was incubated with purified GST-RNF126-WT or GST-RNF126- $\Delta$ e proteins. A GST-pull-down assay was conducted as described. Purified GST-RNF126 protein-WT or GST-RNF126- $\Delta$ e were generated from *Escherichia coli*. GST proteins were detected using a Ponceau S stain (C, E, and F). (G) The exogenous interaction between RNF126 and 14-3-3 $\sigma$  was increased upon ionizing radiation (IR). HEK293T cells were transfected with Flag-RNF126-WT and His-14-3-3 $\sigma$  plasmids. After transfection for 48 h, cells were then irradiated (8 Gy, 2 h). (H) The reciprocal endogenous interaction between RNF126 and 14-3-3 $\sigma$  was increased in a reaction to IR. MCF7 cells were collected after irradiation (8 Gy, 2 h). (I) The region “e” of RNF126 is important for the interaction between RNF126 and 14-3-3 $\sigma$  in response to IR. Flag-RNF126-WT or Flag-RNF126- $\Delta$ e plasmid were co-transfected with His-14-3-3 $\sigma$  in MCF7 and MDA-MB-231 cells. Cells

were irradiated (8 Gy, 2 h). A co-immunoprecipitation (co-IP) assay was performed as outlined in Methods and Materials.

Author Manuscript

Author Manuscript

Author Manuscript

Author Manuscript

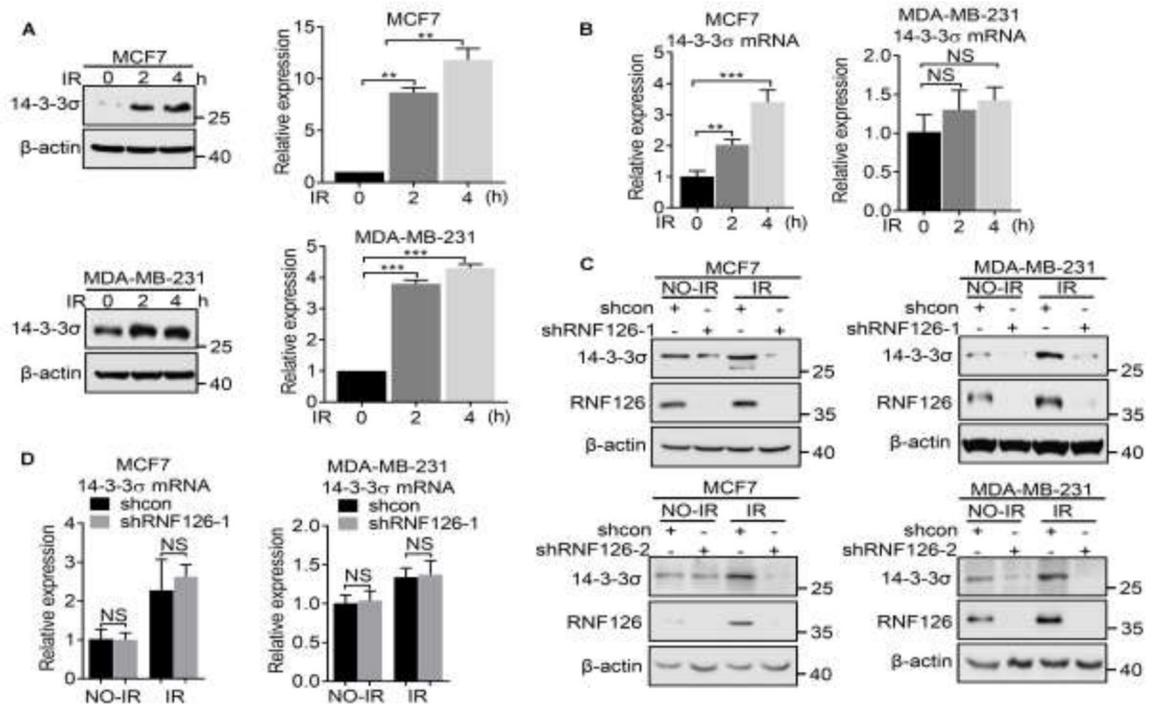


**Figure 3. IR-induced 14-3-3 $\sigma$  protein expression depends on RNF126.**

(A) An increase in the 14-3-3 $\sigma$  protein level was found in response to ionizing radiation (IR; 8 Gy) in MCF7 and MDA-MB-231 cells. The quantification of western blot results is shown (right panel). (B) Ionizing radiation (8 Gy) induced an increase in the 14-3-3 $\sigma$  mRNA level in MCF7 but not MDA-MB-231 cells. (C) Knockdown of RNF126 abrogated IR-induced 14-3-3 $\sigma$  protein expression (8 Gy, 2 h). (D) Knockdown of RNF126 had no effect on the IR-induced mRNA level of 14-3-3 $\sigma$  (8 Gy, 2 h) as measured by quantitative reverse transcription PCR (qRT-PCR). GAPDH mRNA was used to normalize data, which was expressed relative to that of non-irradiated cells. NS, not significant, \*\* $P < 0.01$ , \*\*\* $P < 0.001$ . Data represent the mean  $\pm$  SEM of three independent experiments. One-way ANOVA with Bonferroni post hoc analysis for multiple comparisons was used to check statistical significance. shRNA, short hairpin RNA.

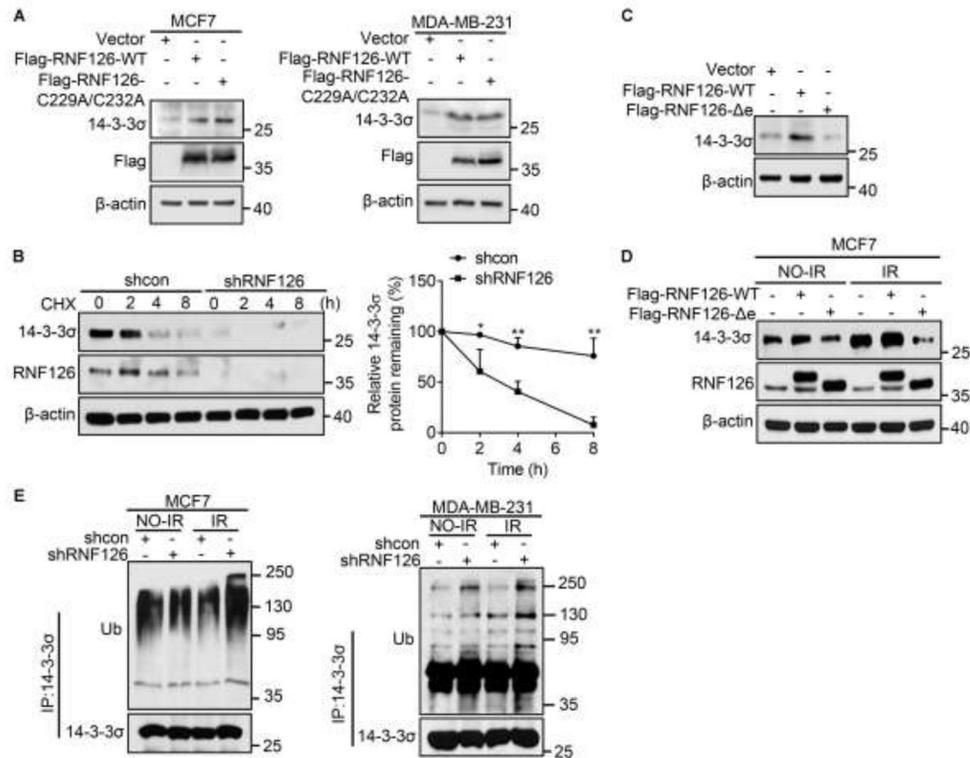


**Figure 4. RNF126 is required for 14–3–3 $\sigma$  protein stability in response to IR.**

(A) MCF7 and MDA-MB-231 cells overexpressing Flag-RNF126-WT and Flag-RNF126-C229A/C232A led to increased expression of 14–3–3 $\sigma$  protein. (B) RNF126 depletion induced an increased 14–3–3 $\sigma$  degradation rate. After treatment with cycloheximide (CHX; 100 mg/mL), MCF7 cells that underwent or did not undergo RNF126 knockdown were collected at various time points (left panel). Three independent experiments were used to quantify the 14–3–3 $\sigma$  protein degradation rate (right panel). Data represent the mean  $\pm$  SEM of three independent experiments. Statistical significance was determined using Student's *t* test. \* $P$  < 0.05, \*\* $P$  < 0.01. (C) Overexpression of Flag-RNF126- $\Delta$ e, a mutant lacking aa130–140 residues, caused decreased 14–3–3 $\sigma$  protein expression compared to Flag-RNF126-WT overexpression. (D) Flag-RNF126- $\Delta$ e transfection decreased 14–3–3 $\sigma$  protein expression, especially in irradiated MCF7 cells (IR). Cell lysates were collected after treatment with or without ionizing radiation (IR; 8 Gy, 2 h). (E) RNF126 deficiency-induced 14–3–3 $\sigma$  ubiquitination (Ub) was increased in response to IR (8 Gy, 2 h). IP, immunoprecipitation; shRNA, short hairpin RNA.

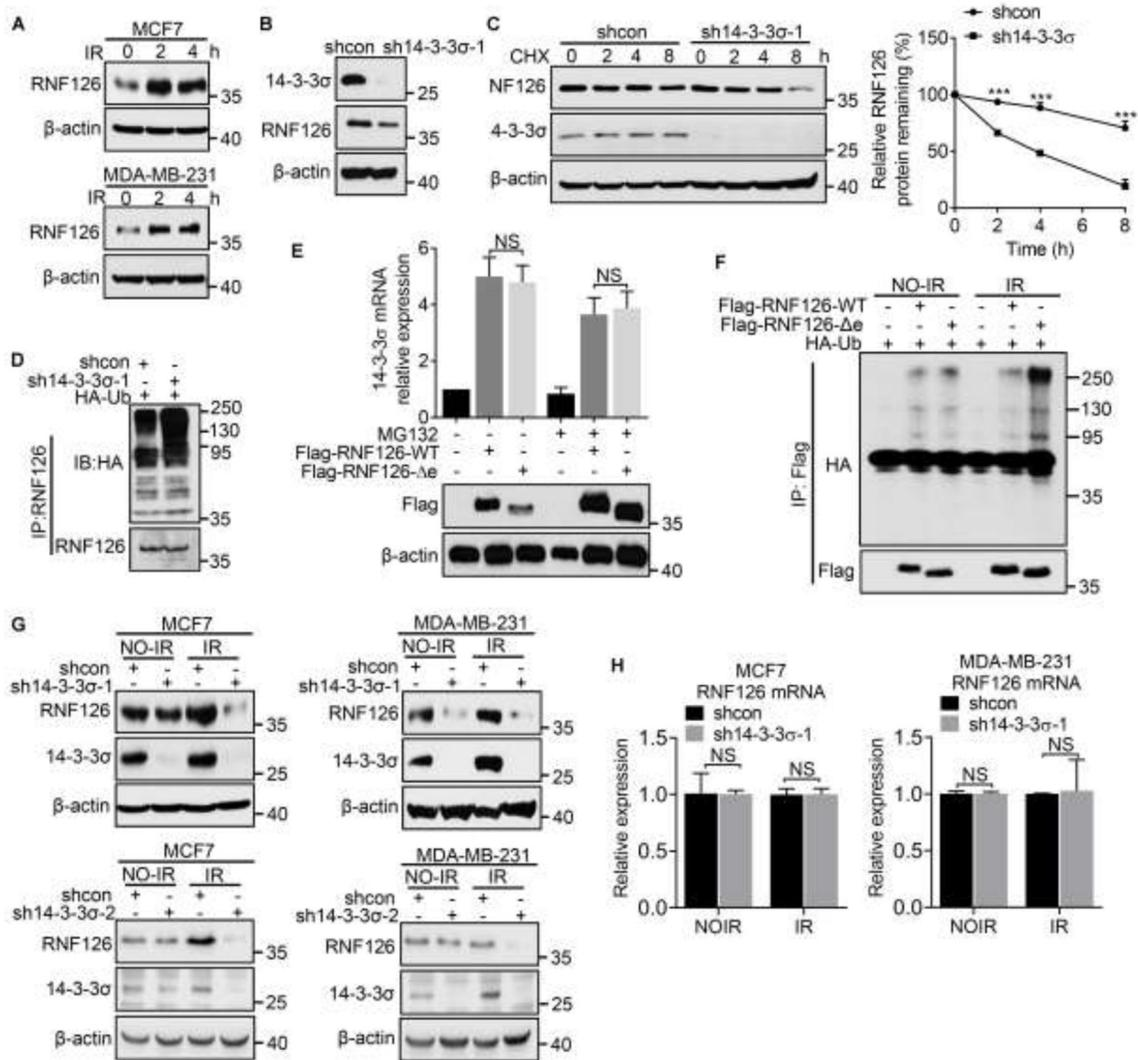


**Figure 5. IR-induced RNF126 is stabilized by binding with 14-3-3 $\sigma$ .**

(A) RNF126 protein expression increased in response to ionizing radiation (IR) in MCF7 and MDA-MB-231 cells. Cells were irradiated and harvested at the indicated time points (8 Gy). (B) Knockdown of 14-3-3 $\sigma$  decreased the RNF126 protein level. (C) A deficiency of 14-3-3 $\sigma$  induced an increased RNF126 degradation rate. MCF7 cells, with or without 14-3-3 $\sigma$  knockdown, were exposed to cycloheximide (CHX; 100 mg/mL). After harvesting at various time points (left panel), the RNF126 protein degradation rate was quantified (right panel). Data represent the mean  $\pm$  SEM of three independent experiments. Statistical significance was determined using Student's *t* test. \*\*\**P* < 0.001. (D) Knockdown of 14-3-3 $\sigma$  induced RNF126 ubiquitination (Ub). (E) RNF126- $\Delta$ e protein expression (lower panel) but not the mRNA level (upper panel) was restored to the levels of the Flag-RNF126-wild type (WT) after MG132 treatment (5  $\mu$ g/mL, 6 h). (F) The ubiquitination level of RNF126- $\Delta$ e was increased compared to RNF126-WT, especially upon irradiation (IR; 8 Gy, 2 h). (G) Knockdown of 14-3-3 $\sigma$  abrogated IR-induced RNF126 protein expression (8 Gy, 2 h). (H) Knockdown of 14-3-3 $\sigma$  had no effect on the IR-induced mRNA level

of RNF126. GAPDH mRNA was used to normalize data, expressed relative to that for non-irradiated cells. Data represent the mean  $\pm$  SEM of three independent experiments. One-way ANOVA with Bonferroni post hoc analysis for multiple comparisons was used to check statistical significance. NS, not significant; HA, HA-Ub; IP, immunoprecipitation; shRNA, short hairpin RNA.

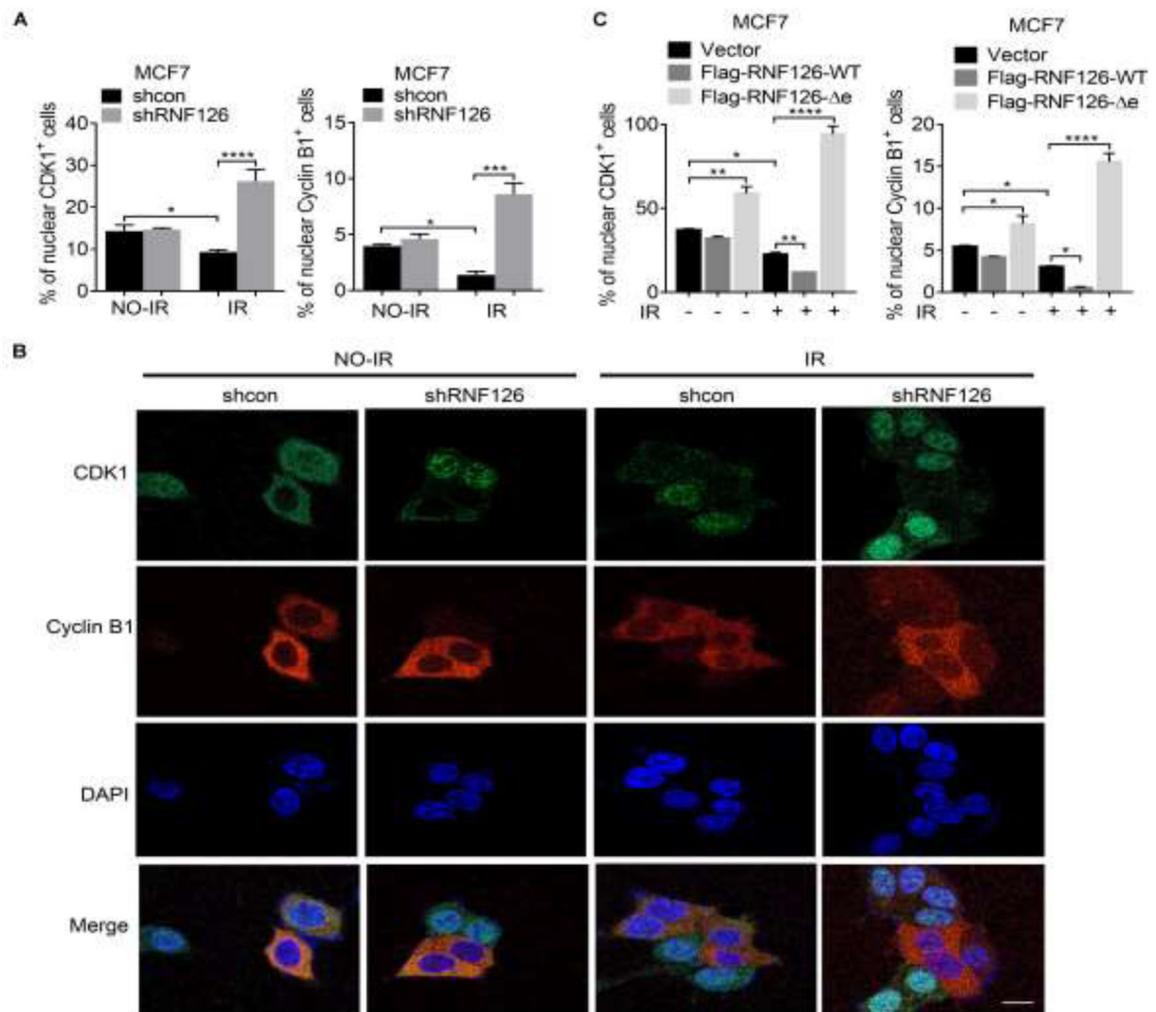


**Figure 6. RNF126 is necessary for sequestering CDK1 and cyclin B1 from the nucleus.** (A) The percentages of cells with positive cyclin B1 and CDK1 staining in MCF7 cells, with or without RNF126 knockdown, in response to ionizing radiation (IR; 8 Gy, 4 h), using an immunofluorescence assay. (B) Representative images of CDK1 and cyclin B1 staining. Scale bar, 100  $\mu$ m. (C) The percentages of cells showing positive CDK1 and cyclin B1 staining. Data represent the mean  $\pm$  SEM of three independent experiments. \* $P$  < 0.05; \*\* $P$  < 0.01, \*\*\* $P$  < 0.001, \*\*\*\* $P$  < 0.0001. One-way ANOVA, followed by a Bonferroni post hoc test, was used to determine statistical significance. shRNA, short hairpin RNA.